Synthesis of Bioinspired Curcuminoid Small Molecules for Solution-Processed Organic Solar Cells with High Open-Circuit Voltage

Florence Archet, Dandan Yao, Sylvain Chambon, Chahine Abbas, Anthony D ' Aléo, Gabriel Canard, Miguel-Armando Ponce-Vargas, Elena Zaborova, Boris Le Guennic, Guillaume Wantz, et al.

Synthesis of Bio-Inspired Curcuminoid Small Molecules for Solution-Processed Organic Solar Cells with High Open Circuit Voltage

Florence Archet,[†] Dandan Yao,[‡] Sylvain Chambon,[†] Mamatimin Abbas,[†] Anthony D'Aléo,[‡] Gabriel Canard,[‡] Miguel Ponce-Vargas,[§] Elena Zaborova,[‡] Boris Le Guennic,[§] Guillaume Wantz,*[†] and Frédéric Fages*[‡]*

[†] Bordeaux INP, Université de Bordeaux, CNRS, IMS UMR 5218, 33400 Talence, France. [‡] Aix Marseille Univ, CNRS, CINaM UMR 7325, 13288 Marseille Cedex 9, France. [§] Institut des Sciences Chimiques de Rennes, UMR 6226 CNRS, Université de Rennes 1, 263 Av. du Général Leclerc, 35042 Cedex Rennes, France.

AUTHOR INFORMATION

Corresponding Author

* boris.leguennic@univ-rennes1.fr. *Guillaume.Wantz@enscbp.fr. * frederic.fages@univ-amu.fr.

ABSTRACT. Borondifluoride complexes of curcuminoid derivatives end-capped with triphenylamine groups were designed for solution-processed bulk-heterojunction organic solar cells. They were obtained very simply in a one-pot synthesis from cheap building blocks.

Compared to push-pull systems based on boron difluoride complexes of hydroxychalcones, curcuminoids present the donor-acceptor-donor electronic structure and exhibit significantly improved chemical and thermal stability and photovoltaic performance. Indeed power conversion efficiency up to 4.14 % and high open-circuit voltage over 1.0 V have been achieved using $PC_{61}BM$ as acceptor.

TOC GRAPHICS

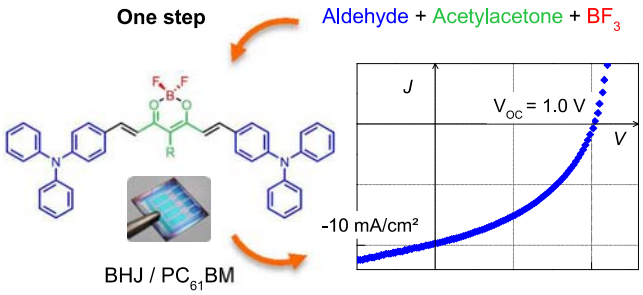

Organic solar cells (OSCs) hold great promise as renewable energy sources that are compatible with low-cost, large-area, solution-processed manufacturing on flexible substrates. Recently, bulk heterojunction (BHJ) OSCs, in which electron-donor and electron-acceptor materials are blended in an active layer, have demonstrated impressive power conversion efficiencies (PCEs) above 11% with polymers[1,2] and around 10%-11% with small molecules.[3,4] Keys to further progress in organic photovoltaics (OPVs) are the rational design of new materials, optimization of BHJ nanoscale morphology, improvement of device architectures, fabrication procedures, and device lifespan. As compared to their polymer counterparts, π-conjugated small molecules with well-defined structures are recognized as versatile donor components for the construction of BHJs using solution processes, such as roll-to-roll printing. To be economically viable, however, industrial application of small-sized molecular donors requires rapid development of cost-effective, green synthetic methodologies that allow the scalable production of high-purity materials.[5,6]

Molecular donors with high molar absorption coefficient and optical band gap matching the solar spectrum are generally designed to feature intramolecular charge transfer by covalently connecting donor (D) and acceptor (A) units in the conjugated backbone. These complex targets are obtained *via* linear multistep syntheses that include desymmetrization and metal-catalyzed cross-coupling of building blocks.[7-10] Contamination may occur, due to trace metals and organic side-products that are difficult to remove. As a result, the synthetic effort is not often rewarded by reasonable overall yields. Actually, recent reports do stress scalability and purification of those conjugated materials as major issues to overcome in the future.[5,6,10-12]

Nature uses conventional nucleophilic reactions to produce structurally complex π-conjugated molecules from simple natural precursors. This led us to envision a bio-inspired synthetic route

in which metal-free ionic reactivity could be exploited for the straightforward generation of borondifluoride complexes of curcuminoids. Those D-A-D molecules are related to the curcumin natural pigment and represent versatile chromophores that capitalize on the strong electron acceptor strength of the chelate moiety containing the Lewis acid boron atom.[13,14] In our initial reports, synthesis was based on two sequential steps, the aldol condensation providing the free ligand followed by BF_2 complexation. Yet simple, this methodology was found to be cumbersome in the case of highly soluble ligands because their thorough purification required repetitive chromatographic steps prior to BF_2 incorporation, thereby limiting drastically the amount of isolated material.

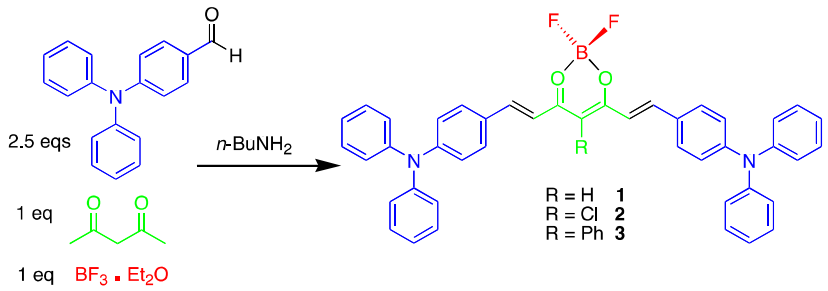

Scheme 1. One-pot synthesis of **1 – 3**

We report herein on three borondifluoride complexes of bis(triphenyl)amine (TPA)-containing curcuminoids, **1 – 3** (Scheme 1) that act as efficient donor materials in solution-processed BHJ solar cells when blended with the electron acceptor [6,6]-phenyl-C_{61}-butyric acid methyl ester ($PC_{61}BM$). We show that the synthesis of compounds **1 – 3** can be made as simple as possible. Indeed, they were obtained easily by mixing TPA carboxaldehyde, acetylacetone (or a *meso*-substituted analogue) and borontrifluoride etherate (2.5:1:1 molar equivalents) in ethylacetate as solvent and in the presence of *n*-butylamine as a base (Scheme 1). We routinely ran batches affording between 700 mg and 1 g of isolated pure material with yields above 70%. We

performed purification by a single flash chromatography column followed by washing the solids with distilled solvents (Supporting Information). Except for compound **2** that is sensitive to protic species in solution owing to the presence of the electron-withdrawing chlorine atom, **1** and **3** were found to be chemically and thermally stable. The thermogravimetric analysis of **1** did not show thermal degradation up to ca. 300 °C (Figure S1). This is an outstanding example of synthesizing a conjugated D-A-D molecule in a one-pot three-component reaction involving cheap commercially available chemicals. According to Roncali *et al.*,[5] compound **1** has a synthetic complexity index (SC) around 9 that represents a record value for efficient OPV materials reported so far.

Crystals of **1** were obtained after slow evaporation of dichloromethane (DCM) solution. They belong to the monoclinic space group P21/n with four molecules in the unit cell (Table S1). The conformation of **1** is not fully planar, with an angle of 33° being noticed between the planes of the aromatic rings belonging to the curcuminoid backbone (Figure 1a). The molecules assemble into one-dimensional π-stacks along the crystallographic b axis with their main molecular planes being oriented parallel to one another and canted by ca. 40° relative to the b axis (Figure S2). Borondifluoride complexes of curcuminoids have a ground-state (GS) dipole moment oriented perpendicularly to the long molecular axis, which explains the observed head-to-tail disposition of the dioxaborine rings. The face-to-face superimposition of the conjugated backbone of **1** occurs with alternate distances between the dioxaborine acceptor planes of 3.54 Å and 3.07 Å, indicating a tight packing of the molecules. Interestingly, along a stack, TPA nitrogen atoms are aligned in straight rows, indicating favorable overlap between TPA moieties of adjacent molecules. Moreover, the crystal lattice contains voids that host highly disordered solvent molecules that could not be resolved.

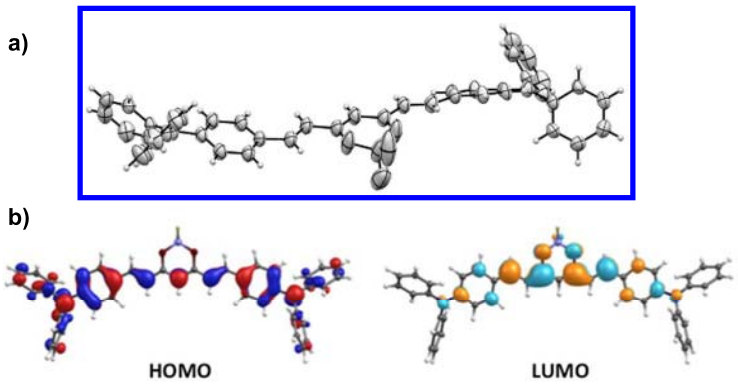

Figure 1. (a) Molecular structure (ORTEP) of compound **1** with displacement ellipsoids drawn at the 50% probability level. (b) Frontier molecular orbitals of **1** (contour threshold: 0.02 a.u.).

Compounds **1 – 3** display strong visible optical absorption in chloroform (CF) solution (Figure 2) and far-red fluorescence emission. The lowest-energy absorption band and fluorescence emission spectra of **1 – 3** are broad and bathochromically shifted in solvents of increasing polarity (Figure S3). The excited state (ES) thus possesses a strong intramolecular charge transfer character with a dipole moment larger than that in the GS, which is confirmed by the Lippert-Mataga analysis of the solvatochromic shifts (Figure S4) and DFT calculations. The presence of the *meso*-phenyl substituent in **3** (λ_{max} = 612 nm) causes a 20-nm red-shift of the absorption relative to **1** (λ_{max} = 594 nm), which was attributed to a conformational effect.[12] Rather, the 50-nm red-shift in the spectrum of **2** (λ_{max} = 642 nm) stems from the enhanced electron accepting strength of the dioxaborine ring featuring the *meso*-chloro substituent, leading to a more polarized D-A-D π-system.

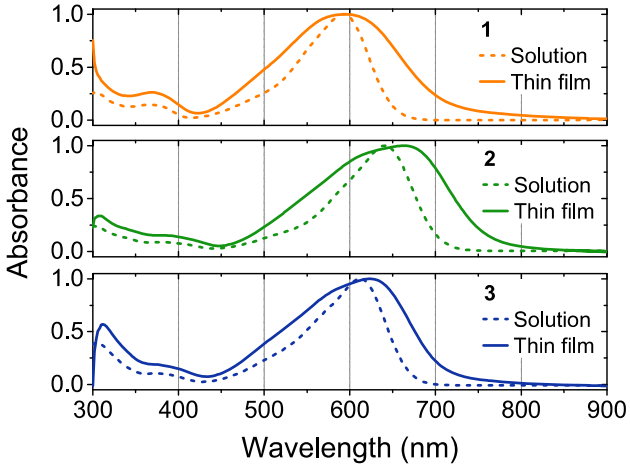

Figure 2. Electronic absorption spectra of **1** (orange), **2** (green) and **3** (blue) in CF solution (solid line) and thin film (dashed line), normalized with absorbance to 1.0.

The three compounds were found to be soluble in CF, chlorobenzene (CB) and o-dichlorobenzene (DCB), allowing spin coating of solutions with concentrations over 10 mg/mL. Compared to solution, thin-film absorption spectra of **1** – **3** are significantly broadened (Figure 2), which indicates the occurrence of π-π interactions as confirmed by the crystal structure of **1**. Unlike **1** (λ_{max} = 592 nm), compounds **2** (λ_{max} = 662 nm) and **3** (λ_{max} = 624 nm) have thin film absorption spectra red-shifted relative to those recorded in solution. This may indicate a better planarization of the curcuminoid backbone or more pronounced interactions in the bulk owing to the presence of the *meso* group. Optical band gaps were estimated from the onset of the thin-film absorption spectra as 1.75 eV, 1.64 eV and 1.75 eV for **1**, **2** and **3**, respectively. With the stronger electron-accepting unit, dye **2** displays a red-shifted onset and thus the narrowest gap (Table S2).

The energy levels of the frontier molecular orbitals (MOs) were estimated from cyclic voltammetry measurements in DCM by taking the onset of the oxidation and reduction waves (Figure S5 and Table S2). The three molecules present a similar value of *ca.* -5.6 eV for the

energy of the highest occupied MO (HOMO) which is compatible with high open-circuit voltage (V_{OC}) when $PC_{61}BM$ is used as acceptor in OSCs.[15] Consistent with the optical properties, the presence of the *meso*-chlorine atom lowers the lowest unoccupied MO (LUMO) of **2** (-4.11 eV) by ca. 130 meV relative to those of **1** and **3** found at -3.96 eV. The positioning of the LUMOs of **1** and **3** is therefore well suited to photoinduced electron transfer into the LUMO of $PC_{61}BM$,[15] which is confirmed by the fluorescence quenching observed in thin-film blends (*vide infra*).

DFT/TD-DFT calculations were performed on **1 – 3** (see computational details in ESI). The three molecules display identical contour plots of HOMOs and LUMOs (Figures 1b and S6). HOMOs are mostly delocalized over the lateral groups with a significant contribution of TPA phenyl rings, whereas LUMOs are mainly located on the central dioxaborine acceptor moiety. The lowest energy (vertical) transition band consists mainly in HOMO → LUMO charge transfer transition (Table S3). This is consistent with the electronic density difference plots (Figure S6) that provide the difference between the electronic density of the lowest singlet ES and the GS. The energy level values obtained with optical, electrochemical, and theoretical approaches follow the same trends. For **1** and **3**, GS and ES dipole moments amount to almost 11 D and to over 12 D, respectively (Table S4). Overall dipoles moments are weakened for **2** (GS: 8.8 D; ES: 10.2 D) as a result of the local antiparallel dipole moment of the C(*meso*)-Cl bond. These data are consistent with the solvatochromic absorption and fluorescence properties.

BHJ OSCs were fabricated using the following architecture: ITO/PEDOT:PSS/**1**–**3**:$PC_{61}BM$/Ca/Al (Supporting Information) and tested under 100 mW/cm² illumination. Donor:$PC_{61}BM$ blends (50:50 w/w) were spin-coated from CB. The devices based on **2** and **3** present lower power conversion efficiencies (PCE = 0.9% and 1.1% respectively) compared to **1** that reached 3.1% (Figure S7 and Table S5). The main difference arises from lower short-circuit

current density (J_{SC} = 8.9, 4.3 and 5.0 mA/cm² for **1**, **2** and **3** respectively). Hole mobilities (μ_h) were determined from organic field-effect transistors (OFETs, Table S6). Results show that **2** and **3** present much lower μ_h than **1**, consistent with a higher J_{SC} for the latter. Therefore, only devices based on **1**:$PC_{61}BM$ were further optimized.

Figure 3 presents the impact of **1**:$PC_{61}BM$ blend ratio on J_{SC} and PCE. With increasing $PC_{61}BM$ concentration from 15 to 40 w%, J_{SC} gradually rises up to 8 mA/cm^2.

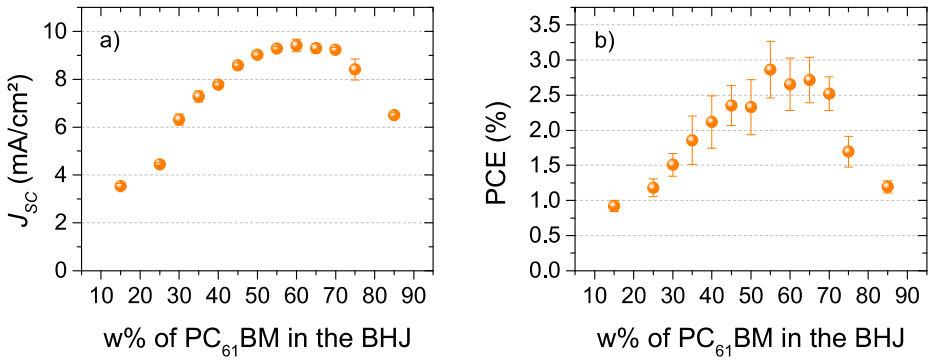

Figure 3. (a) J_{SC} and (b) PCE of BHJ OSCs based on **1**:$PC_{61}BM$ with different blend ratios. Film thickness: 72-85 nm.

Almost total fluorescence quenching occurs at 40 w% of $PC_{61}BM$ (100 % quenching above 50 w%, Figure S8). As a result, with further addition of $PC_{61}BM$ up to 70 w%, J_{SC} levels off at 8-9 mA/cm^2. Beyond this concentration, J_{SC} drops off because of the reduced optical absorption in **1**. The low values of the fill factor (FF < 40%, Table S7) may stem from the unbalanced charge carrier mobilities (Table S6), μ_h being found smaller than electron mobility. Devices with a weight ratio in a range from 55 to 65 w% of $PC_{61}BM$ provided the best value of PCE close to 3%.

To explain the change of J_{SC} as a function of the blend ratio, we investigated **1**-$PC_{61}BM$ blend morphologies using tapping mode atomic force microscopy (AFM, Figure S9). We observed the formation of large domains for low concentrations of $PC_{61}BM$ that disappear when $PC_{61}BM$

reaches 35 w%. Between 35 and 75 w%, smooth layers and small domains with similar sizes are observed and the morphology is independent of the blend composition. At low $PC_{61}BM$ content, because of their strong GS permanent dipole, molecules **1** self-assemble via electrostatic interactions as the main driving force.[16,17] Therefore large domains of **1** are likely to prevail resulting in strong geminate recombination and, in turn, in a low J_{SC}. From 35 w% to 75 w% of $PC_{61}BM$, the observed morphology is likely to favor exciton dissociation, leading to higher J_{SC}. In that case, because both **1** and $PC_{61}BM$ possess a high dipole moment,[18] **1**:$PC_{61}BM$ dipolar interactions may assist the formation of the intimately mixed blends. Such intermolecular interactions would also account for the red-shift of the thin film absorption ($\Delta\lambda$ = + 10 nm) noticed above 35 w% of $PC_{61}BM$ (Figure S10).

External quantum efficiencies (EQE) recorded at different **1**:$PC_{61}BM$ blend ratios (Figure 4) support the previous observations and also provide further interesting information. As expected, increasing $PC_{61}BM$ loading from 30 to 70 w% leads to an increase of the contribution of both donor and acceptor materials. However, the EQE response of **1** starts decreasing beyond 70 w%. Interestingly, at 50 w% of $PC_{61}BM$, a new band appears at 450 nm in the EQE spectrum and grows with a further increase of $PC_{61}BM$. This contribution can be attributed to the occurrence of $PC_{61}BM$ aggregates.[19] Above this threshold concentration, the formation of larger $PC_{61}BM$ aggregates would create the conduction pathways for the electrons and improve the charge transport. Finally, the optimum performance is found for a balance between intermixed state for high exciton dissociation rate (< 70% $PC_{61}BM$) and large domains that favor charge transport (> 50% $PC_{61}BM$).

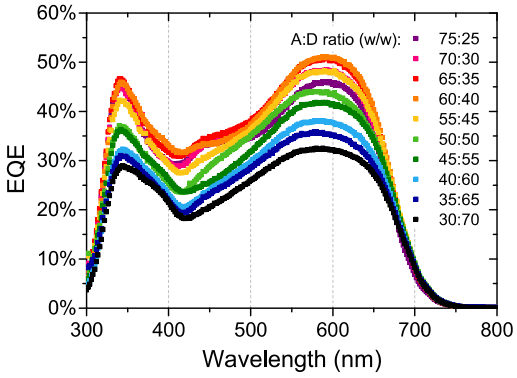

Figure 4. EQE curves of devices based on **1**:$PC_{61}BM$ with different blend ratios.

In order to improve further the morphology, we fabricated BHJ OSCs using CF, CB or DCB as solvents to spin coat the **1**:$PC_{61}BM$ blend (ratio 35:65 w/w). Compared to devices spun from CB and DCB, CF-processed OSCs show a slightly improved J_{SC} (Figure 5). Interestingly, the use of CF also leads to an increase of V_{OC} up to 1.0 V (Figure 5 and Table S8). The use of CF as a more volatile solvent influences the organization of both **1** and $PC_{61}BM$ and the degree of phase separation. This is supported by EQE spectra showing a higher contribution at 450 nm, associated with $PC_{61}BM$ aggregates (Figure S11).

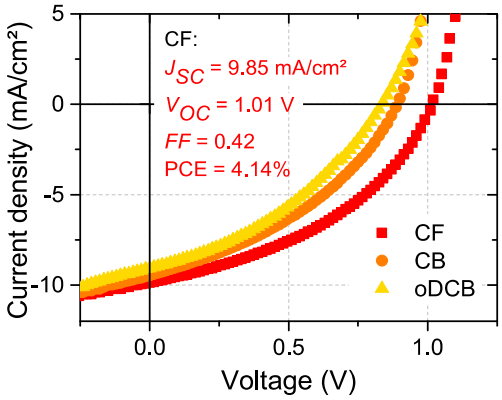

Figure 5. *J-V* curves under 100 mW/cm² illumination of BHJ OSCs made with **1**:$PC_{61}BM$ (35:65 w/w) spin-coated from CF (red), CB (orange) and DCB (yellow).

Moreover, phase images of AFM measurements performed on blends processed from CF, CB and DCB clearly show differences in morphology (Figure S12). DCB seems to give an intermixed active layer. Using CB leads to the formation of D and A domains which appear still too small to create efficient pathways for charges. Interestingly, using CF as a processing solvent, the D and A domains are larger and efficient percolation pathways are expected to build up. Such kind of morphology reduces bimolecular recombination losses, which could explain the higher V_{OC}.[20] These results suggest that fast drying of the layer is favorable to the formation of an optimized BHJ with enhanced photocurrent. Finally, among the devices prepared in this study, the best performance was obtained at 65 w% $PC_{61}BM$ using CF as the processing solvent, with J_{SC} = 9.85 mA/cm², V_{OC} = 1.01 V and FF = 0.42 giving an overall PCE of 4.14%. In contrast, V_{oc} values obtained for boron difluoride complexes of hydroxychalcones as donor materials did not exceed 0.63 V.[14]

In summary, we report the fabrication and initial characterization of BHJ OSCs based, for the first time, on borondifluoride complexes of curcuminoid derivatives as molecular donors and $PC_{61}BM$ as the acceptor. The synthesis of compounds **1 – 3** is remarkably simple, cost effective and environmentally friendly and results in a record low synthetic complexity index (SC = 9 for **1**). Compared to related materials based on push-pull hydroxychalcone derivatives,[14,21] curcuminoids feature a D-A-D extended π-conjugated system leading to significant overlap between TPA terminal moieties in the crystal. Moreover, unless it contains an electron withdrawing group such as the chlorine atom in **2**, the acetylacetonate ligand moiety of the curcuminoids provides dioxaborine chelates that are more stable, both chemically and thermally, with respect to those obtained with hydroxychalcones. Therefore the results show the high

potential of those D-A-D structures as molecular scaffolds on which to base the design of optimized donor materials for BHJ OSCs.

ASSOCIATED CONTENT

General methods, synthetic procedures, NMR spectra, UV−vis and fluorescence spectra, CV measurements, OFETs and OSCs fabrication and characterization data, single-crystal data, DFT calculations, crystallographic data (CIF).

AUTHOR INFORMATION

Notes

The authors declare no competing financial interest.

ACKNOWLEDGMENT

This work was supported by the French National Research Agency (ANR) ("Chalcones" Project, ANR-14-CE05-0035-01). This research used resources of the GENCI-CINES/IDRIS. We thank Dr. Michel Giorgi for single-crystal DRX measurements. Authors are thankful to the ANR as part of the « Investissements d'avenir » program (reference: ANR-10-EQPX-28-01/Equipex ELORPrintTec).

REFERENCES

(1) Zhao, J.; Li, Y.; Yang, G.; Jiang, K.; Lin, H.; Ade, H.; Ma, W.; Yan, H. Efficient Organic Solar Cells Processed from Hydrocarbon Solvents. *Nat. Energy* **2016**, *1*, 15027.

(2) Park, K. H.; An, Y.; Jung, S.; Park, H.; Yang, C. The Use of an n-Type Macromolecular Additive as a Simple yet Effective Tool for Improving and Stabilizing the Performance of Organic Solar Cells. *Energy Environ. Sci*. **2016**, *9*, 3464-3471.

(3) Kan, B.; Li, M.; Liu, F.; Wan, X.; Yunchuang, W.; Wang, N.; Long, G.; Yang, X.; Feng, H.; Zuo, Y. *et al*. A Series of Simple Oligomer-like Small Molecules Based on Oligothiophenes for Solution-Processed Solar Cells with High Efficiency. *J. Am. Chem. Soc.* **2015**, 137, 3886-3893.

(4) Deng, D.; Zhang, Y.; Wang, Z.; Zhu, L.; Fang, J.; Xia, B.; Wang, Z., Lu, K.; Ma, W.; Wei, Z. Fluorination-Enabled Optimal Morphology Leads to over 11% Efficiency for Inverted Small-Molecule Organic Solar Cells. *Nat. Commun*. **2016**, 7, 13740.

(5) Po, R.; Roncali, J. Beyond Efficiency: Scalability of Molecular Donor Materials for Organic Photovoltaics. *J. Mater. Chem. C*. **2016**, *4*, 3677-3685.

(6) Osedach, T. P.; Andrew, T. L.; Bulović, V. Effect of Synthetic Accessibility on the Commercial Viability of Organic Photovoltaics. *Energy Environ. Sci*. **2013**, 6, 711-718.

(7) Ni, W.; Wan, X.; Li, M.; Wang, Y.; Chen, Y. A–D–A Small Molecules for Solution-Processed Organic Photovoltaic Cells. *Chem. Commun*. **2015**, *51*, 4936-4950.

(8) Carsten, B.; Szarko, J. M.; Son, H. J.; Wang, W.; Lu, L.; He, F.; Rolczynski, B. S.; Lou, S. J.; Chen, L. X.; Yu, Y. Examining the Effect of the Dipole Moment on Charge Separation in Donor–Acceptor Polymers for Organic Photovoltaic Applications. *J. Am. Chem. Soc.* **2011**, *133*, 20468-20475.

(9) Liu, X.; Sun, Y.; Hsu, B. B. Y.; Lorbach, A.; Qi, L.; Heeger, A. J.; Bazan, G. C. Design and Properties of Intermediate-Sized Narrow Band-Gap Conjugated Molecules Relevant to Solution-Processed Organic Solar Cells. *J. Am. Chem. Soc*. **2014**, *136*, 5697-5708.

(10) Coughlin, J. E.; Henson, Z. B.; Welch, G. C.; Bazan, G. C. Design and Synthesis of Molecular Donors for Solution-Processed High-Efficiency Organic Solar Cells. *Acc. Chem. Res*. **2014**, *47*, 257-270.

(11) Wessendorf, C. D.; Schulz, G. L.; Mishra, A.; Kar, P.; Ata, I.; Weidelener, M.; Urdanpilleta, M.; Hanisch, J.; Mena-Osteritz, E.; Lindén, M. *et al*. Efficiency Improvement of Solution-Processed Dithienopyrrole-Based A-D-A Oligothiophene Bulk-Heterojunction Solar Cells by Solvent Vapor Annealing. *Adv. Energy Mater*. **2014**, *4*, 1400266.

(12) Usluer, Ö.; Abbas, M.; Wantz, G.; Vignau, L.; Hirsch, L.; Grana, E.; Brochon, C.; Cloutet, E.; Hadziioannou, G. Metal Residues in Semiconducting Polymers: Impact on the Performance of Organic Electronic Devices. *ACS Macro Letters* **2014**, *3*, 1134-1138.

(13) Felouat, A.; D'Aléo, A.; Fages, F. Synthesis and Photophysical Properties of Difluoroboron Complexes of Curcuminoid Derivatives Bearing Different Terminal Aromatic Units and a meso-Aryl Ring. *J. Org. Chem*. **2013**, 78, 4446-4455.

(14) Chambon, S.; D'Aléo, A.; Baffert, C.; Wantz, G.; Fages, F. Solution-Processed Bulk Heterojunction Solar Cells Based on BF_2–Hydroxychalcone Complexes. *Chem. Commun*. **2013**, *49*, 3555-3557.

(15) Scharber, M. C.; Sariciftci, N. S. Efficiency of Bulk-Heterojunction Organic Solar Cells. *Progress Polym. Sci.* **2013**, 38, 1929-1940.

(16) Arjona-Esteban, A.; Krumrain, J.; Liess, A.; Stolte, M.; Huang, L.; Schmidt, D.; Stepanenko, V.; Gsänger, M.; Hertel, D.; Meerholz, K. *et al*. Influence of Solid-State Packing of Dipolar Merocyanine Dyes on Transistor and Solar Cell Performances. *J. Am. Chem. Soc.* **2015**, *137*, 13524-13534.

(17) Takacs, C. J.; Sun, Y.; Welch, G. C.; Perez, L. A.; Liu, X.; Wen, W.; Bazan, G. C.; J. Heeger, A. J. Solar Cell Efficiency, Self-Assembly, and Dipole–Dipole Interactions of Isomorphic Narrow-Band-Gap Molecules. *J. Am. Chem. Soc*. **2012**, *134*, 16597-16606.

(18) de Gier, H. D.; Jahani, F.; Broer, R.; Hummelen, J. C.; Havenith, R. W. A. Promising Strategy To Improve Charge Separation in Organic Photovoltaics: Installing Permanent Dipoles in PCBM Analogues. *J. Phys. Chem. A* **2016**, *120*, 4664-4671.

(19) Cook, S.; Ohkita H.; Kim, Y.; Benson-Smith, J. J.; Bradley, D. D. C.; Durrant, J. R. A Photophysical Study of PCBM Thin Films. *Chem. Phys. Lett*. **2007**, *445*, 276-280.

(20) Ali, M.; Abbas, M.; Shah, S. K.; Tuerhong, R.; Generosi, A.; Paci, B.; Hirsch, L.; Gunnella, R. Realization of Solution Processed Multi-Layer Bulk Heterojunction Organic Solar Cells by Electro-Spray Deposition. *Org. Electron.* **2012**, 13, 2130-2137.

(21) D'Aléo, A.; Heresanu, V.; Giorgi, M.; Le Guennic, B.; Jacquemin, D.; Fages, F.; NIR Emission in Borondifluoride Complexes of 2′-Hydroxychalcone Derivatives Containing an Acetonaphthone Ring. *J. Phys. Chem. C* **2014**, *118*, 11919-11927.